



EUROfusion

WPJET2-CPR(18) 18849

Yushan Zhou et al.

**The effect of gyration on the deposition
of Beryllium and Deuterium at rough
surface on the divertor tiles with
ITER-like-wall in JET**

Preprint of Paper to be submitted for publication in Proceeding of
23rd International Conference on Plasma Surface Interactions in
Controlled Fusion Devices (PSI-23)



This work has been carried out within the framework of the EUROfusion Consortium and has received funding from the Euratom research and training programme 2014-2018 under grant agreement No 633053. The views and opinions expressed herein do not necessarily reflect those of the European Commission.

This document is intended for publication in the open literature. It is made available on the clear understanding that it may not be further circulated and extracts or references may not be published prior to publication of the original when applicable, or without the consent of the Publications Officer, EUROfusion Programme Management Unit, Culham Science Centre, Abingdon, Oxon, OX14 3DB, UK or e-mail Publications.Officer@euro-fusion.org

Enquiries about Copyright and reproduction should be addressed to the Publications Officer, EUROfusion Programme Management Unit, Culham Science Centre, Abingdon, Oxon, OX14 3DB, UK or e-mail Publications.Officer@euro-fusion.org

The contents of this preprint and all other EUROfusion Preprints, Reports and Conference Papers are available to view online free at <http://www.euro-fusionscipub.org>. This site has full search facilities and e-mail alert options. In the JET specific papers the diagrams contained within the PDFs on this site are hyperlinked

The effect of gyration on the deposition of beryllium and deuterium at rough surface on the divertor tiles with ITER-like-wall in JET

Y. Zhou^a, H. Bergs aker^a, P. Petersson^a, G. Possnert^b, J. Likonen^c and JET contributors^{*}

EUROfusion Consortium, JET, Culham Science Centre, Abingdon, OX14 3DB, UK

*^aDepartment for Fusion Plasma Physics, School of Electrical Engineering,
Royal Institute of Technology, S-10405 Stockholm, Sweden*

^bUppsala Universitet, Tandem Laboratory, S-75105 Uppsala, Sweden

^cVTT Technical Research Centre of Finland, P.O.Box 1000, FIN-02044 VTT, Finland

** See the author list of "X. Litaudon et al 2017 Nucl. Fusion 57 102001*

yushan@kth.se

Abstract

Previous experimental results from micro beam analyses on divertor tiles, through 2011-2012 and 2013-2014 operations, showed that the deuterium retention and the beryllium impurity deposition were nonuniform on the rough surface. Frequently, the Be and D were accumulated within pits, cracks and valleys in the range of $\sim 10 \mu\text{m}$ to $\sim 100 \mu\text{m}$ and selectively at side slopes within larger pits. Column growth in deposited layers was also observed in determined directions with respect to the magnetic field.

Modelling suggested the trajectory of carbon ions in the boundary sheath led to an inhomogeneous ion flux on rough surfaces (a few micro meters). Therefore the motion of ions and the impinging on surface could be potential reasons for the nonuniform deposition. In this work, in order to figure out the effect of the ion gyro motion on Be and D deposition on the real divertor topography, a simulation of ion trajectories in the plasma boundary has been made with the isothermal plasma assumption. The surface topography was measured with the focus stacking technique on photos from optical microscopy.

Ion beam analysis data suggested that surface D accumulated on the top stage of sample while Be stayed on the 10-20 μm stages. Gyro-motion of D could explain this accumulation on the top qualitative but overestimated the D amount in lower stage ($\geq 20 \mu\text{m}$ from the top of the sample). While experimental results for Be agreed with the simulation data only on the stages located at $\approx 20 \mu\text{m}$ from the top. Influence on electric field model from the surface structure and sputtering of Be by D should be considered for improvements of the simulation.

Introduction

Interactions between plasma and vessel wall generates critical issues in present fusion devices. The erosion of wall materials limits the life time of plasma facing components (PFC). Eroded particles (impurities) can migrate from initial positions to remote areas through the scrape-off layer and eventually re-deposit on surfaces somewhere in the machine, especially on the deposition dominated areas at divertor tiles in a tokamak. Deposited layers grow gradually during plasma operation mixing with hydrogen particles which can be retained in the deposited film by the co-deposition process. The substantial accumulation of hydrogen in deposited layers can bring problems to the tritium limitation in ITER and to the economic efficiency for a reactor [1].

However, both the erosion of wall materials and the deposition of hydrogen shows non-uniform pattern in micro meter scale over the surface of PFCs in fusion machines with metal wall or carbon wall. The surface facing towards the magnetic field suffered more serious erosion than the surface facing away from magnetic field [2, 3] and deuterium was found to be accumulated at the valley-like structures [4, 5]. Those non-uniform patterns complicate the estimation of the total amount of hydrogen retention in vessel wall which could generate large uncertainty. The weak adhesion of hydrogen rich deposited films to the substrate may generate dust particles, which is another critical issue for operating fusion device.

In order to understand this non-uniform pattern, surveys for the surface structures and the behavior of particles have been made recently. For structures, bubbles sized hundreds of nanometers were observed in stratified deposited layer, which potentially related to the deuterium retention and layer cracking [6, 7]. Simulations for transport of impurities, with a given background plasma, and simulation for deposition of impurities on artificial surface indicated that the roughness of surface increased the amount of deposited impurities [8]. Also, the topography of surfaces altered the electric field next the surface and impacted the trajectory of particles, contributing to the non-uniform deposition pattern through particle-in-cell simulation [9]. Besides, the surface structures could provide a shadowing effect to prevent the adjacent surfaces from being touched by the incident plasma flux, which protects the deposition layer locally [2].

Since the experimental data from different devices and simulations on artificial surfaces suggest that the surface topography may play a significant role in the deposition process, it would be interesting to compare the deposition results and simulation on the same sample which experienced the exposure to plasma. In this paper, the micro ion beam was used to observe the distribution of deuterium and beryllium deposition over a sample surface which came from the JET ITER-like wall (JET-ILW) project, with beryllium in the main chamber wall and tungsten and tungsten coated carbon fibre composite (CFC) in the divertor. The sample surface structure was measured by the stacking method for photos from an optical microscope. On this surface structure, simulation for tracing the trajectories of particles from the plasma to the surface, penetrating the magnetic presheath and Debye sheath, was made using MATLAB functions.

Methods

The experiments for ion beam analysis (IBA) and optical microscopy were carried out in Uppsala University. Micro ion beam with $^3\text{He}^{2+}$ at 3MeV was applied to measure the deuterium and beryllium amount on the sample, by nuclear reactions $\text{D}(^3\text{He},\text{p})^4\text{He}$ and $\text{Be}(^3\text{He},\text{p})^{11}\text{B}$ [10,

11]. The Sample (tungsten coated CFC) located at the upper vertical part of Tile1 (1/8) [12] with around 10 μm deposited layer on the top after the 2013-2014 operation [13]. Details of detectors can be found in [14]. The linear size of ion beam spot was about 5-10 μm and the current stayed in the range of hundreds of pA during the measurements (in total $2.3 \times 10^{11} \text{ sr} * \text{particles}$). The beam spot scanned the interesting region on the sample surface marked by an attached copper grid. Data from every scanned point was stored in a 256*256 matrix. The energy spectrum from the whole scanned region was fitted by SIMNRA 6. Combining the matrix and fitting results, the elemental map of the D and Be spatial distributions can be acquired.

The surface structure was measured by the focus stacking on sample photos from optical microscopy. The stacking method is a digital image processing which merges photos from different focal depths for the same object since only part of areas on the object can be focused in single photo. Therefore, by controlling the focal depth, the surface structure can be measured. In this paper the focal depth of the microscope was controlled by moving the stage in steps and each step was 4 μm . By taking photos on different focal depths, the sample was transferred into layers with depth resolution of 4 μm and eventually merged into a three dimensional image containing the structure information. By carefully overlaying the structure image with the distribution map of D and Be, we could compare the topography and experimental data of deposition distribution.

The simulation focused on the trajectories of particles in the plasma and sheath until it reached the sample surface. The motion of particles is dominated by the gyro-motion and $\mathbf{E} \times \mathbf{B}$ drift. The surface structure data used in the simulations came from the focus stacking result. For simplification, the boundary plasma was divided into three regions as shown in Fig.1 in which the plasma with only magnetic field stays on the top followed by the magnetic presheath (MPS) and Debye sheath (DS)[15]. In the coordinates in Fig.1, the bottom of the sample is located at the XY plane with roughness following the Z axis. The magnetic field is inclined to the XY plane with angle $\delta = 5^\circ$ and the electric field in the sheath is perpendicular to XY plane.

The basic assumption in the simulation was that the background plasma stayed in isothermal condition with equivalent electron and ion temperature. The magnetic and electric fields in the plasma and within the different sheaths were constant and uniform. The magnetic field strength B , electron density and temperature came from the experimental data in reference. The charge number for Be was +2 and the time step in trajectory calculation was 10^{-11}s with 10^5 input particles.

The particle trajectory began on a point in the plasma determined by three parameters: a, f, g . Variables f and g are linear random number limited by the size of sample surface in simulation in order to allow the impact positions to cover the whole simulation region. Parameter a represented the distance from initial point to the entrance of magnetic presheath as shown in Fig.1. It was randomly chosen from zero to a_0 which indicated the distance a particle can travel when it finishes a full gyro-motion orbit in plasma.

$$a_0 = \frac{2\pi}{\omega} V_{para} \quad (1)$$

ω is the gyro-motion frequency with $B = 2.7 \text{ T}$ [16] and V_{para} is the velocity component parallel to magnetic field. It can be derived from the Bohm criterion [17] by ion sound speed with electron and ion temperature $T_e = T_i = 7 \text{ eV}$ [15, 18].

$$V_{para} = c_s = \sqrt{\frac{k(T_e + T_i)}{m_i}} \quad (2)$$

The perpendicular velocity V_{perp} was the thermal velocity which was randomly taken from Maxwell distribution. The distribution was determined by the electron temperature and depended on atomic mass. By randomly choosing the distance between initial position and the entrance, ions in the plasma moved with a full or partial gyro-orbit before they impact the entrance of the MPS with different impact angles and velocities. The calculation of trajectory in the sheath used those angles and velocities as input data.

Having entered the sheath, ions were exposed to additional drift and acceleration from electric field \mathbf{E} generated by the potential drop in sheath region. The total potential drop V in the two sheaths is shown in equation (3) together with potential drop in MPS V_{MPS} in equation (4) [15]. The electric field in each sheath was derived from the ratio of potential drop to the width of sheath in equation (6) and (7). ω_{ci} stands for gyro-frequency of ion and the electron density $n_e = 2.5 \times 10^{20} \text{ m}^{-3}$ [18].

$$V = \frac{kT_e}{2e} \ln\left(\frac{2\pi m_e}{m_i} \left(1 + \frac{T_i}{T_e}\right)\right) \quad (3)$$

$$V_{MPS} = \frac{kT_e}{e} \ln(\cos(90 - \delta)) \quad (4)$$

$$V_{DS} = V - V_{MPS} \quad (5)$$

$$L_{MPS} \approx \sqrt{6} \left(\frac{c_s}{\omega_{ci}}\right) \sin(90 - \delta) \quad (6)$$

$$L_{DS} = \sqrt{\epsilon_0 T_e / e^2 n_e} \quad (7)$$

$$E_{DS} = \frac{V_{DS}}{L_{DS}} \sim 10^6 \text{ V/m}, \quad E_{MPS} = \frac{V_{MPS}}{L_{MPS}} \sim 10^4 \text{ V/m} \quad (8)$$

$$m \frac{d\mathbf{r}}{dt} = q(\mathbf{E} + \mathbf{v} \times \mathbf{B}) \quad (9)$$

The time dependent position $\mathbf{r}(t)$ and velocity $\mathbf{v}(t)$ of a particle was acquired by solving the equation of motion (9). The MATLAB symbolic toolbox gave the analytical solution for this equation with $\mathbf{B}(0, B_y, B_z)$ and $\mathbf{E}(0, 0, E_z)$. The impact position and the velocity of particle were stored in a six column matrix for further estimation of the probability density function (PDF). The z component of surface, z and y components of particles impact positions were transferred into PDF for comparison.

Results

Fig.2 represents the sample surface used in the simulation as a greyscale image. The spatial resolution in the z direction is 4 μm and 2-3 μm in x and y direction. The shades of grey show the depth of the structure from the top to the bottom. The maximum value in the grey-scale bar indicates the top of surface ($\approx 105 \mu\text{m}$) and the minimum means the bottom. The major part of the surface can be considered as perpendicular to the toroidal magnetic field B_Φ with several flat stages varied from 95 μm to 70 μm in depth, accompanied with some deep holes $\leq 60 \mu\text{m}$.

Three rectangles with dashed line mark the regions from which the simulation data was compared with IBA results.

Fig.3 shows the surface deuterium distribution over the surface from IBA data. The term 'surface' means the top layer of deposited film with thickness around $1.6 \mu\text{m}$ in terms of pure Be. The color bar shows the amount of deposited D. By comparing to the greyscale image, it was found that surface D mainly accumulated on the stage in depth $\approx 95 \mu\text{m}$ from $350 \mu\text{m}$ to $500 \mu\text{m}$ in y direction. Since the structure indicated by white plays a minor role over the whole region, it is convenient to consider the stage in depth around $95 \mu\text{m}$ as the 'top' of the region. Therefore, the surface D can be thought of as accumulated on the top of the surface. The distribution of Be in Fig.4 was derived from the total amount of Be instead of that of the surface. The color image of Be only shows the areas with areal density greater than $1 \times 10^{20} \text{ atoms/cm}^2$. Unlike D, Be stays on the lower stages, i.e. in the depth around $85 \mu\text{m}$ to $70 \mu\text{m}$ from $450 \mu\text{m}$ to $650 \mu\text{m}$ in y direction. Besides, Be was also found in the deep hole with depth $\leq 60 \mu\text{m}$ at ($X \approx 360 \mu\text{m}$, $Y \approx 550 \mu\text{m}$) while D accumulated on the adjacent higher stages.

Fig.5, Fig.6, and Fig.7 show the simulation results from the regions marked by rectangles. Subsets named as (A) represent the PDF for the z component of the surface (black dotted line) and impact positions for both D (blue dashed line) and Be (red solid line). The PDF for the y component of impact positions are described in the upper part of subsets (B), together with the surface structure from the corresponding region in the lower part. Difference in PDF from z component suggests that gyro-motion of particle brings non-uniform impact positions for both D and Be on all three regions.

Fig.5-(A) shows that the simulated deuterium deposition in region (1) has higher probability on structures at $Z1 \approx 97\text{-}90 \mu\text{m}$, $Z2 \approx 85\text{-}80 \mu\text{m}$, and $Z3 \approx 80\text{-}75 \mu\text{m}$. $Z1$ responds to the slope from $600 \mu\text{m}$ to $630 \mu\text{m}$ in Fig.5-(B) and PDF of y component has relative high values on this position. This agrees with the IBA result on Fig.3. $Z2$ relates to the area on $Y \approx 570\text{-}585 \mu\text{m}$ and $Y \approx 667\text{-}690 \mu\text{m}$. On both areas, IBA data suggest the D accumulation as well. However, there is no IBA data for the accumulation in $Y \approx 645\text{-}665 \mu\text{m}$ region as predicted by the peaks in PDF of y which responds to surface with depth in $Z3$. For Be, prediction from PDF of y only agrees with the IBA data on $Y \approx 667\text{-}690 \mu\text{m}$. On other areas in region (1), simulation overestimated the probability of Be deposition.

PDF results from region (2) are shown in Fig.6. The PDF of the y component of D is roughly uniform varying around 0.004. PDF on z suggests D may accumulate on $Z \approx 90\text{-}80 \mu\text{m}$. On the corresponding area on $Y \approx 490\text{-}580 \mu\text{m}$, IBA data show relatively high D amount on a smaller area with $Y \approx 520\text{-}570 \mu\text{m}$. IBA data in Fig.3 also indicate that D accumulated on $Y \approx 650 \mu\text{m}$ and PDF of y ($\approx 0.006\text{-}0.008$) on the same position can response to it. But the simulation data on $Z \leq 80 \mu\text{m}$, at $Y \approx 600 \mu\text{m}$, cannot find the relative experimental results. For Be results, the high value of Be deposition on region (2) appears on $Y \approx 530\text{-}550 \mu\text{m}$ and $Y \approx 470\text{-}510 \mu\text{m}$ from IBA data in Fig.4. PDF on y component in Fig.6-(B) shows some peaks ($\approx 0.008\text{-}0.01$) on the similar areas while PDF peak (≥ 0.012) on $Y \approx 620 \mu\text{m}$ overrates the probability.

Region (3) locates on the top stage with substantial surface D. In Fig.7-(B), the continuous curve on PDF of y ($\approx 0.006\text{-}0.008$) from $Y \approx 420 \mu\text{m}$ to $Y \approx 500 \mu\text{m}$ responds to the accumulation on this area. However, the predicted high value for surface D from PDF of y on $Y \approx 500\text{-}520 \mu\text{m}$ cannot be found through IBA results in Fig.3. The same happens to the PDF of y ($\approx 0.004\text{-}0.008$) as well on $Y \approx 320\text{-}370 \mu\text{m}$ region with $Z \leq 80 \mu\text{m}$. As for the Be simulation result on region (3) in Fig.7-(B), it suggests a large amount of Be on the top stage, with PDF of y

($\approx 0.008-0.012$), at $Y \approx 420-500 \mu\text{m}$ which cannot be found in Fig.4. But the accumulation of Be in $Y \approx 320-370 \mu\text{m}$ could be predicted by the PDF of y ($\approx 0.004-0.008$) in the similar region.

Discussion

Comparison between the IBA results and simulation data on three regions suggests gyro-motion of D with uniform electric field in each sheath can qualitatively explain the accumulation of surface D on the stop stage at the sample in depth around $95 \mu\text{m}$ with the coordinates in simulation. The simulation also agrees with experimental data on the stages located in depth around $85 \mu\text{m}$ ($\approx 10-15 \mu\text{m}$ from the top of sample), Therefore for the surface D, gyro-motion may play a significant role for the deposition pattern. However, the simulation overestimates the D amount of regions in depth $\leq 80 \mu\text{m}$ ($\geq 20 \mu\text{m}$ from the top of the sample). One potential reason for it would be the surface structure strongly influences the electric field in those regions. As shown in [9], the distribution of electric potential above rough surface follows the surface structure and the potential drop increases when surface consists of a larger valley. In this case, the electric field which is perpendicular to the isopotential surface bends to the local surface instead of staying in the vertical position as assumed in the simulation. The improvement for the electric field model should be taken into account in the future.

The accumulation of total Be can be explained partially by the gyro-motion simulation on the regions in depth around $80 \mu\text{m}$ ($\approx 20 \mu\text{m}$ from the top of sample). On other areas, the simulation overestimated the probability, especially on which surface D accumulated exemplified by the area with $Y \approx 600-630 \mu\text{m}$ in region (1) and area with $Y \approx 420-500 \mu\text{m}$ in region (3). Both two areas stay on the top stage with depth around $95 \mu\text{m}$. The gyro-motion of D in this area could lead to impact of D occurring frequently, which could generate the Be sputtering with the sputtering yield in the range from 10^{-3} to 10^{-2} atom per incident ion [19].

Be self-sputtering may contribute to the lower Be content as well since the sputtering yield stays in the magnitude from 10^{-2} to 10^{-1} [19, 20]. Measurement for Be self-sputtering and D-Be sputtering in [21] shows that the incident angle of impinging ions effect the sputtering yield as well. The incident angle distribution is affected by other plasma density, magnetic field strength and inclined angle etc. [22].

The simulation in the paper did not consider the reflection of D from Be and Be from Be. The reflection coefficients of Be from Be is around 10^{-3} and it is convenient to neglect the reflected Be [20]. The reflection of D may need to be considered in the future as improvement since the coefficient is about 10^{-1} . The reflected D may promptly re-deposited at the adjacent area and this progress may change the local deposition pattern.

Base on the discussions above, it appears that the cooperation between surface structure and sputtering results the non-uniform deposition pattern. The sample structure in this work partially carried over from the roughness of coating layer. For the future device without coating, results from this work could still provide some suggestions for estimating the fuel retention since the plasma-wall interactions will create several kinds of structures. And the accumulation of Be on deeper regions also imply that when depressed area appears the deposited Be could fill up this area since it may suffers less sputtering from D in long-term operation.

Conclusions

A He beam in micro meter scale was applied for measuring the D and Be amount on a sample from JET-ILW. The topography of the sample surface was obtained by the focus stacking

method on piles of photos from the optical microscope and it was the input surface data in the simulation for gyro-motion of D and Be. Impact positions of D and Be on the surface were compared with the distribution of surface D and Be over the sample surface on three selected regions. IBA data suggested that surface D accumulated on the top stage of sample while Be stayed on the 10-20 μm stages. Gyro-motion of D could explain this accumulation on the top qualitative but overestimated the D amount in deeper stage. A possible reason for the overestimate may come from the electric field model in simulation which did not reflect the influence from surface structure. Experimental results for Be agreed with the simulation data only on the stages located at $\approx 20 \mu\text{m}$ from the top. To explain this, the sputtering of deposited Be by D should be considered since the surface D accumulated on the region with less Be.

Acknowledgment

This work has been carried out within the framework of the EUROfusion Consortium and has received funding from the Euratom research and training programme 2014-2018 under grant agreement No 633053. The views and opinions expressed herein do not necessarily reflect those of the European Commission.

References

- [1] J. Roth, et al., *J. Nucl. Mater.*, 390 (2009) 1-9.
- [2] K. Schmid, et al., *NUCL FUSION*, 50 (2010) 11.
- [3] M. Mayer, et al., *Physica Scripta*, 2007 (2007) 5.
- [4] H. Bergsåker, et al., *Nucl Instrum Meth B*, 332 (2014) 266-270.
- [5] H. Bergsåker, et al., *J. Nucl. Mater.*, 463 (2015) 956-960.
- [6] M. Tokitani, et al., *Fusion Engineering and Design*, 116 (2017) 1-4.
- [7] S. Masuzaki, et al., *Physica Scripta*, 2017 (2017) 014031.
- [8] S. Y. Dai, et al., *Plasma Physics and Controlled Fusion*, 55 (2013).
- [9] W. Hu, et al., *Nucl Mater Energy*, 12 (2017) 313-317.
- [10] V. K. Alimov, et al., *Nucl Instrum Meth B*, 234 (2005) 169-175.
- [11] E. Wolicki, et al., *Physical Review*, 116 (1959) 1585.
- [12] H. Bergsåker, et al., *Physica Scripta*, 2016 (2016) 014061.
- [13] A. Widdowson, et al., *Nucl Mater Energy*, 12 (2017) 499-505.
- [14] Y. Zhou, et al., *Nucl Mater Energy*, 12 (2017) 412-417.
- [15] P. C. Stangeby, ed., *CRC Press*, 2000. 61- 105.
- [16] M. Mayer, et al., *Physica Scripta*, T167 (2016) 9.
- [17] K.-U. Riemann, *Journal of Physics D: Applied Physics*, 24 (1991) 493.
- [18] S. Brezinsek, et al., *NUCL FUSION*, 53 (2013) 13.
- [19] J. Roth, et al., *J. Nucl. Mater.*, 165 (1989) 199-204.
- [20] W. Eckstein, *MPI-Garching Report IPP 9/132*, (2002) 316.
- [21] M. Stamp, et al., *J. Nucl. Mater.*, 415 (2011) S170-S173.
- [22] I. Borodkina, et al., *Contributions to Plasma Physics*, 56 (2016) 640-645.

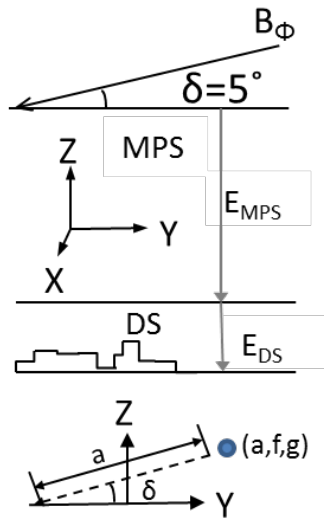


Fig.1 Sketch for the coordinate in simulation. Particle passed through the plasma and penetrates the magnetic presheath and Debye sheath before eventually impact the sample surface. Magnetic field inclined with 5° and electric fields in each sheath were perpendicular to xy plane.

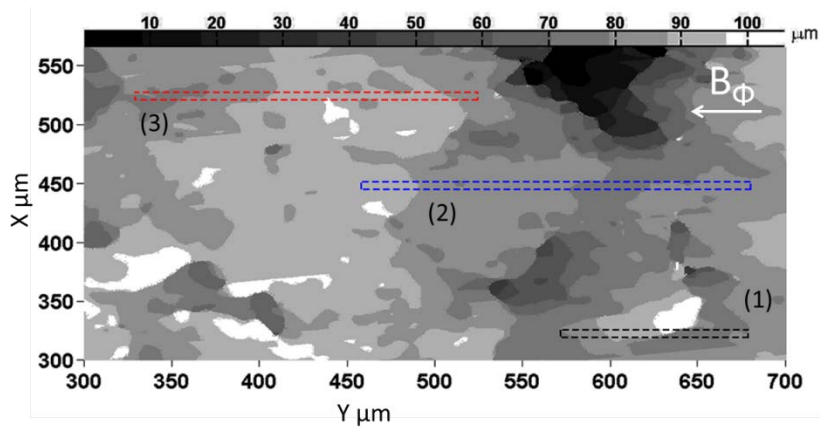


Fig.2 Image for the surface topography by the focus stacking method on photos from optical microscope. The spatial resolution in z direction is $4\ \mu\text{m}$ and $2\text{-}3\ \mu\text{m}$ in x and y direction. The maximum value in grey-scale bar indicates the top of surface ($\approx 105\ \mu\text{m}$) and the minimum means the bottom.

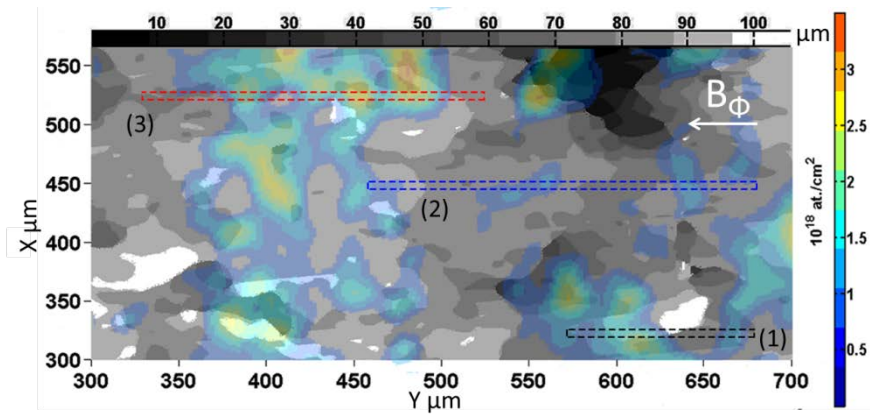


Fig.3 Surface deuterium distribution from top layer of deposited film with thickness around $1.6 \mu\text{m}$ in terms of pure Be. It was overlaid with the greyscale image of topography. The surface D mainly accumulated on the stage in depth $\approx 95 \mu\text{m}$ from $350 \mu\text{m}$ to $500 \mu\text{m}$ in y direction.

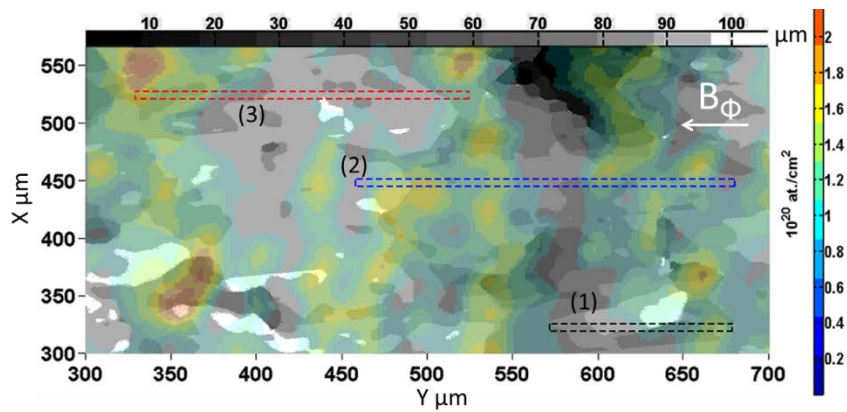


Fig.4 The distribution of Be derived from the total amount of Be instead of that of surface. The color image of Be only shows the areas with areal density are greater than 1×10^{20} atoms/cm². Be stays on the lower stages and the deep hole with depth $\leq 60 \mu\text{m}$.

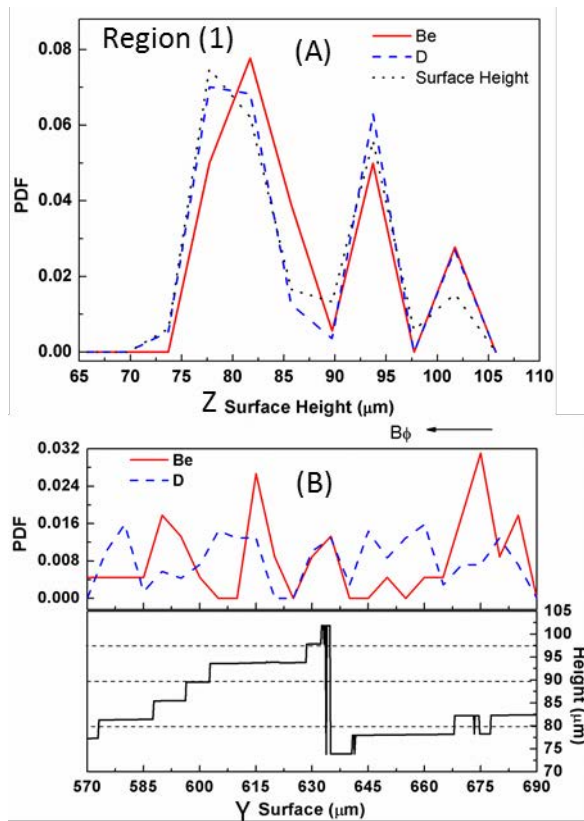


Fig.5 The simulated deuterium deposition in region (1) . For D, the simulation results on the slop from 600 μm to 630 μm agree with the IBA result. But there is no corresponding IBA data for the accumulation in $Y \approx 645\text{-}665 \mu\text{m}$ region as predicted by the peaks in PDF of y. For Be, prediction from PDF of y only agrees with the IBA data on $Y \approx 667\text{-}690 \mu\text{m}$.

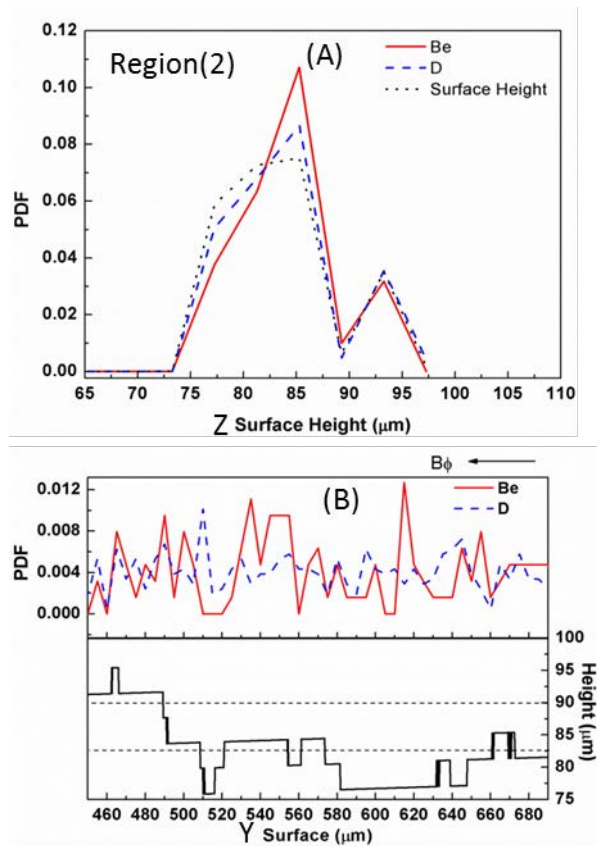


Fig.6 Simulation results on region (2). The PDF of y component of D is roughly uniform. Simulation for D on $Y \approx 490-580 \mu\text{m}$, agree with IBA data shows relative high D amount on a smaller area. But the simulation data on $Z \leq 80 \mu\text{m}$, at $Y \approx 600 \mu\text{m}$, cannot find the relative experimental results. For Be results, the high value of Be deposition on region (2) appears on $Y \approx 530-550 \mu\text{m}$ and $Y \approx 470-510 \mu\text{m}$ from IBA and PDF on y component shows some peaks on the similar areas.

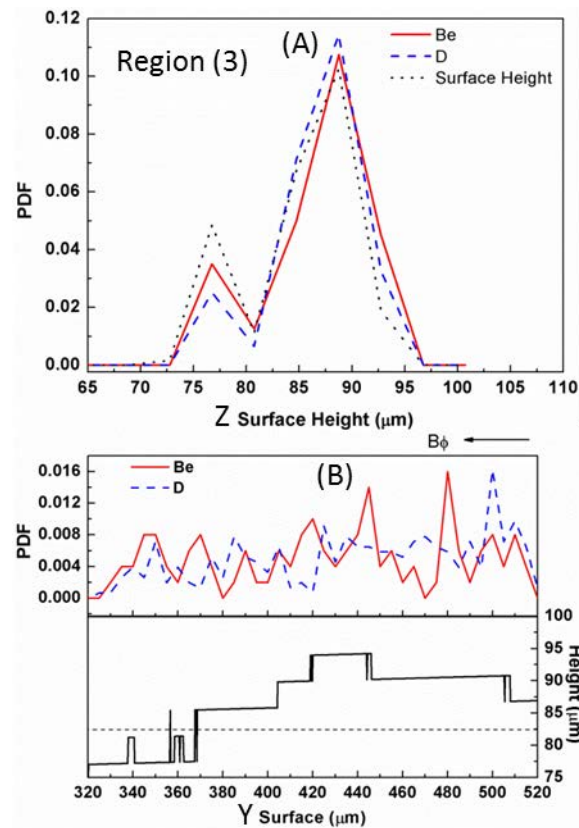


Fig.7 Simulation results on region (3). The continue curve on PDF of y from $Y \approx 420 \mu\text{m}$ to $Y \approx 500 \mu\text{m}$ responses to the accumulation on this area. However, the predicted high value for surface D from PDF of y on $Y \approx 500\text{-}520 \mu\text{m}$ cannot be found through IBA results. The Be simulation result on region (3) suggests a large amount of Be on the top stage which cannot be found in IBA results.